Semiconductor Physics, Quantum Electronics & Optoelectronics, 2008. V. 11, N 2. P. 124-131.

PACS 73.40.Cg, Gk, Lq

Direct current transport mechanisms in n-InSe/p-CdTe heterostructure

P.M. Gorley[1], I.V. Prokopenko[2], Z.M. Grushka[1], V.P. Makhniy[1], O.G. Grushka[1], O.A. Chervinsky[1]
[1]*Yu. Fedkovych Chernivtsi National University*
2, Kotsyubynsky str., 58012 Chernivtsi, Ukraine
Phone: +38 03722 46877, fax: +38 03722 46877, e-mail: semicon@chnu.cv.ua
[2]*V. Lashkaryov Institute of Semiconductors Physics, NAS of Ukraine*
41, prospect Nauky, 03028 Kyiv, Ukraine, phone: +38 044 5254449, e-mail: prokop@isp.kiev.ua

Abstract. The authors created *n*-InSe/*p*-CdTe heterojunction by deposition over optical contact, investigated temperature evolution of its current-voltage dependences under the forward bias, and determined the prevailing current transport mechanisms in the structure. It was shown that misfit dislocations at the boundary between the semiconductors form a stable periodic structure acting as slow recombination centers for the carriers. The properties of the material suggest promising application perspectives for *n*-InSe/*p*-CdTe heterojunction, especially for the devices working at high temperatures and elevated radiation.

Keywords: heterojunction, *n*-InSe/*p*-CdTe, optical contact, current-voltage curve, misfit dislocations, current transport mechanisms, band diagram.

Manuscript received 28.02.08; accepted for publication 15.05.08; published online 30.07.08.

1. Introduction

Development of modern solid state electronics requires creation of efficient devices for operation in extreme conditions, in particular, under the elevated temperatures, significant radiation flux, etc. One of the best structures suiting these applications is *n*-InSe/*p*-GaSe heterojunction, which, according to Refs. [1-4], may efficiently substitute traditional photodiodes based on silicon for aggressive condition applications after proper technology fine-tuning and use of the materials with the optimal parameters. The main peculiarities of the heterojunction mentioned are caused by its layered semiconductor components with unique physical and chemical properties [5]. In particular, the dominating Van der Waals bounding between the layers allows to obtain the plates with the mirror-like and practically ideal surface simply chipping off the crystals. Due to the completeness of chemical bonds the resulting surface will be characterized with high passivity towards the environment, featuring the low concentration of surface defects [3, 5]. The advantages of the heterojunction based on the layered semiconductors also include the possibility to form them by deposition over optical contact [1], resulting in strong adhesion approaching bulk durability of the contacting materials. This method is also beneficial because it does not require high-temperature treatment, avoiding formation of additional boundary layers and cross-doping effects [6].

It is worth mentioning that *n*-InSe/*p*-GaSe structures are quite expensive as they contain rare elements such as gallium. Therefore, it is a timely and important task to find the compounds alternative to *p*-GaSe, which could be significantly cheaper and, at the same time, will be characterized by well-developed technology, so they can be successfully used together with *n*-InSe for creation of efficient heterojunction with the stable parameters for aggressive working environments. Our research proved that one of the best material choice for the mentioned applications includes wide-band A_2B_6 semiconductors, in particular *p*-CdTe, which is the most perspective (and generally used) for detectors of ionizing radiation [7]. However, in contrast to *n*-InSe/*p*-GaSe, the heterojunctions of *n*-InSe/*p*-A_2B_6 are characterized with significant mismatch of lattice constants [8, 9]. Probably due to this, heterojunction *n*-InSe/*p*-A_2B_6 was less investigated in comparison with *n*-InSe/*p*-A_3B_6 structures. In particular, to the best of our knowledge, only one paper [10] is devoted to the studies of electrical parameters of *n*-InSe/*p*-CdTe junction. The investigated structure was formed by *p*-CdTe film sputtering (final thickness of about 0.5 μm and specific resistivity $\rho \approx 200$ Ohm·m) over *n*-InSe crystals ($\rho \approx 3$ Ohm·m). The authors of Ref. [10] also suggested the energy diagram for *n*-InSe/*p*-CdTe hetero-

© 2008, V. Lashkaryov Institute of Semiconductor Physics, National Academy of Sciences of Ukraine

junction, accounting for thermal emission and tunneling currents, as well as recombination processes at the interface.

In this paper, we present investigation results concerning the technology for *n*-InSe/*p*-CdTe heterojunction created by deposition over an optical contact, together with the detailed study of temperature influence on current-voltage curves (CVC) under forward-bias of the structure. We also discuss the peculiarities of dominating current transport mechanisms through the rectifying contact, showing that the height of the heterojunction potential barrier is determined with the energy level created by misfit dislocations at the semiconductor junction. In the considered temperature range (250-330 K), this energy level may act as a slow carrier recombination center. It was also shown that under a small forward bias the slopes of CVC for *n*-InSe/*p*-GaSe and *n*-InSe/*p*-CdTe heterojunctions practically coincide, proving that strong optical contact in *n*-InSe/*p*-CdTe system lowers the requirements of lattice parameter matching due to the mutual weakening of misfit dislocations with the opposite signs.

2. Research objects and methodology

To produce the heterojunction under study, we used monocrystalline samples of CdTe and InSe grown by the Bridgman method from the melt of stoichiometric content without introduction of any doping impurities. As a significant part of Bridgman-grown InSe crystals belongs to ε-polytype [11], we have used the lattice constants $a \equiv a_n = 4.05$ Å and $c = 16.93$ Å [12]. Introduction of impurity in a small quantity causes formation of γ- and δ-polytypes of InSe [11]; however, the resulting lattice constant difference do not exceed 1.5 % (i.e., $a_n = 4.002$ Å for γ-polytype [13]). The similar case can be also observed for other layered crystals [12]. Most probably, namely due to this reason the majority of the literature devoted to the studies of layered semiconductors (or creation of diode structures based on them) usually do not mention the exact crystalline modification of the materials studied. Bulk Bridgman-grown CdTe crystallizes in sphalerite lattice, described with some discrepancy in different references concerning its lattice constant *a*: 6.477 [14], 6.481 [15], 6.4822 Å [16]. For our calculations, we used the average value $a(\text{CdTe}) \equiv a_p = 6.48$ Å.

At the room temperature, CdTe samples featured *p*-type conductivity with the hole concentration $p_0 \cong 1\cdot10^{14}\,\text{cm}^{-3}$ and mobility $\mu_p \cong$ 50-80 $\text{cm}^2/(\text{V·s})$; InSe samples were of *n*-type with the concentration of the majority carriers $n_0 \cong 3\cdot10^{15}\,\text{cm}^{-3}$ and the mobility $\mu_n \cong$ 800-950 $\text{cm}^2/(\text{V·s})$. The density of states $N_{C(V)}(T) = 2.51\cdot\left(\frac{m_{n(p)}}{m_0}\cdot\frac{T}{300}\right)^{3/2}\cdot10^{19}\,\text{cm}^{-3}$ and the Fermi level position $E_{\text{F}n(p)} = k_0 T \ln(N_{C(V)}/n(p))$ [16] were calculated using the effective mass of electrons in InSe $m_{n\perp} = 0.156\ m_0$ [8] and heavy holes in CdTe $m_p = 0.81\ m_0$ [8] (where m_0 is the free electron mass) in the approximation of parabolic dispersion relation and non-degenerated statistics of the carrier gas, yielding the values $N_C \approx 1.55\cdot10^{18}\,\text{cm}^{-3}$, $N_V \approx 1.83\cdot10^{19}\,\text{cm}^{-3}$, $E_{\text{F}n} \cong 0.15$ eV and $E_{\text{F}p} \cong 0.31$ eV for $T = 300$ K.

Heterojunction substrates were made of 4×4×0.5 mm *p*-CdTe samples; the high surface purity of the material was ensured by the technology described in Ref. [17]. The *n*-type plates of InSe, several square millimeters in area, were obtained by chipping off thin (~10 μm) layers from the monocrystalline samples. They had the mirror-smooth surface, thus not requiring any additional treatment. Resistivity measurements yielded the values $R \approx 300$ Ohm for *p*-CdTe samples and $R \approx 0.1$ Ohm for *n*-InSe under the room temperature for the given parameters and linear dimensions of the base materials.

Heterojunctions *n*-InSe/*p*-CdTe were created by pressing a thin elastic *n*-InSe plate against *p*-CdTe substrate until they stuck together forming an optical contact. All the preparation procedures mentioned above concerning the preparation of individual heterojunction components were carried right before creation of the structure. The ohmic contacts for *n*- and *p*-regions of heterojunction were made by spray-deposition of In and Ni films, respectively.

Current-voltage curves of *n*-InSe/*p*-CdTe heterojunctions were measured at the constant current in the temperature range 250 to 330 K, featuring a pronounced diode character with the rectification coefficient equal to 300-400 at the room temperature and the voltage $U = 1$ V. Illuminating heterojunction from the side of CdTe (light flux power 80 mW/cm^2), we detected open circuit voltage of 0.4 V. Analysis of CVC for the structure was performed using the software "Solar Cell Simulator", developed by the authors for modeling of current transport processes in various semiconductor structures [18].

3. Results and discussion

3.1 Structure of defects in the contact plane of n-InSe/p-CdTe junction

Analysis of the obtained CVC proved their small difference from the case typically observed for the semiconductor heterostructures. In particular, it was found that under a significant bias ($U > 1.0$-1.5 V depending on the temperature T) the CVC of *n*-InSe/*p*-CdTe heterojunction obeys the power function

$$I \approx C\cdot(U - U_0)^m, \quad (1)$$

with the cut-off voltage $U_0 = 0.20 \pm 0.10$ V and power $m = 1.54 \pm 0.06$. The validity of the expression (1) is confirmed by the presence of linear branches on $I^{2/3} = f(U)$ curve (Fig. 1). The obtained value of *m* highlights the significant role played by carrier recombination for the current transport through the semiconductor junction [19, 20]. The position of the

© 2008, V. Lashkaryov Institute of Semiconductor Physics, National Academy of Sciences of Ukraine

energy level for the recombination centers $E_r = 0.25 \pm \pm 0.02$ eV was determined from the slope of power-law segment of CVC at the constant voltage in $\ln I = f(10^3/T)$ plot [16, 19] (see the inset to Fig. 1). The obtained value of E_r positively correlates with the position of background impurity level $E_V + 0.24$ eV in non-doped *p*-CdTe [21, 22].

Another important detail can be revealed comparing CVC of the heterojunction studied (Fig. 2, hollow circles) with the data presented in Ref. [10] (Fig. 2, triangles) and CVC of *n*-InSe/*p*-GaSe heterojunction [4] (Fig. 2, solid circles). As one can see, these curves are qualitatively similar in the wide ranges of the forward bias ($U < 1.5$ V). It is worth mentioning that current flowing through the junction increases exponentially with voltage for a small bias ($0 < U < 0.8$ V) for all the studied temperatures. The slope of CVC $S = d\ln I/dU$ significantly increases with temperature, yielding the values $S = 0.21 \pm 0.02$ for $U < 0.5$ V and room temperature. It was shown that the magnitude of S display no dependence both on structure manufacturing methodology and on semiconductor conductivity type (*n*- or *p*-type).

The latter result is quite unexpected, the given lattice mismatch

$$r = 2\cdot\left| a_p - a_n \right| / (a_p + a_n) \qquad (2)$$

for *n*-InSe/*p*-CdTe heterojunction overcoming significantly the same parameter for *n*-InSe/*p*-GaSe structure (46.15 and 7.56 %, respectively; the latter value is obtained for $a(\varepsilon\text{-GaSe}) \equiv a_p = 3.755$ Å [12]). At the same time, there could be many misfit dislocations in *n*-InSe/*p*-CdTe heterojunction, the distance between which can be expressed as [23, 24]

$$l = a_p a_n / \left| a_p - a_n \right| . \qquad (3)$$

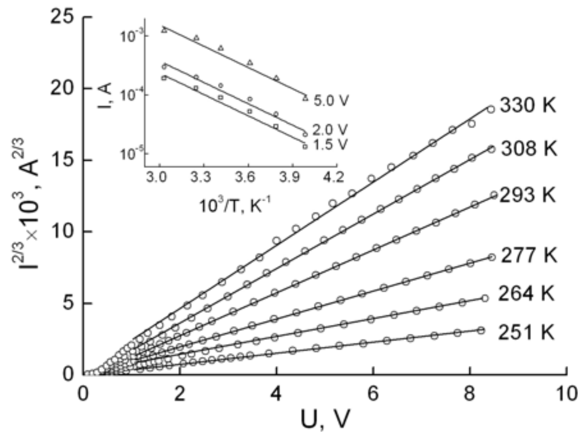

Fig. 1. $I^{2/3} = f(U)$ curves for forward-biased *n*-InSe/*p*-CdTe heterojunctions under different temperatures. The inset shows current as a function of inverse temperature at a constant voltage.

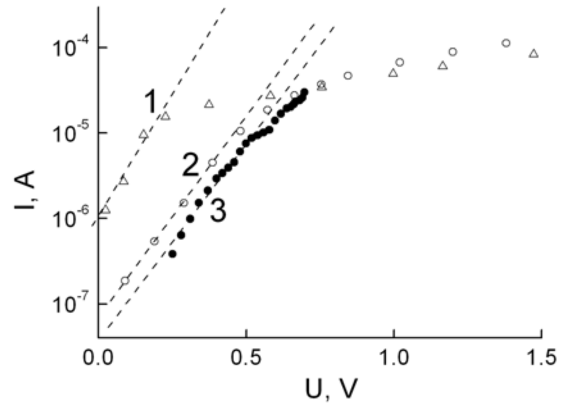

Fig. 2. Experimental CVC for the *n*-InSe/*p*-CdTe heterojunctions measured at the room temperature: 1 – data from Ref. [11], 2 – our results, 3 – data from Ref. [4].

Using the crystalline lattice constant 10.8 Å, one can see that for the case of *n*-InSe/*p*-GaSe heterojunction the number of such dislocations is significantly lower due to the large distance between them, $l \cong 51.55$ Å.

Our analysis have shown that for *n*-InSe/*p*-CdTe structure the misfit dislocations may have two types, being formed by broken bonds of either InSe, or CdTe, which will result in their opposite signs [25]. As crystalline lattice constants of base semiconductors obey the expression a_p(CdTe) / a_n(InSe) = 1.6, one should expect that *n*-InSe/*p*-CdTe junction plane will feature a translation symmetry structure with a period $a_{st} = 5a_p = 8a_n = 3l = 32.4$ Å, corresponding to the “elementary cell” of a defect structure inside the junction investigated. The schematic distribution of misfit dislocations within the distance a_{st} is presented in Fig. 3. It is important to emphasize that each such “cell” is composed by two areas and has an inversion center coinciding with misfit dislocation created by non-saturated InSe samples. Neglecting the interaction between the closest-neighboring dislocations of the opposite sign, we calculated the distance between the centers yielding the values proportional to those shown in Fig. 3, scaled by a coefficient $l_0 \equiv a_{st}/40 = 0.81$ Å. As the distances l_0 and $2l_0$ between misfit dislocation centers are smaller than $a_n/2$, one should expect dislocation cylinder overlapping, increasing dislocation annihilation probability. The latter phenomenon will mutually weaken the partial tensions in the “elementary cell”, which will become a single stable formation [23, 26-27].

Naturally, as it follows from the geometrical model discussed above (Fig. 3), accounting for interacting dislocations (which due to the smallness of the distances between the dislocation centers should be considered in the frame of elasticity theory [25]) will change the distribution of defects. But, taking into account purely physical analysis, one will also come to the conclusion that the defect “cell” will be stable in this case, too.

© 2008, V. Lashkaryov Institute of Semiconductor Physics, National Academy of Sciences of Ukraine

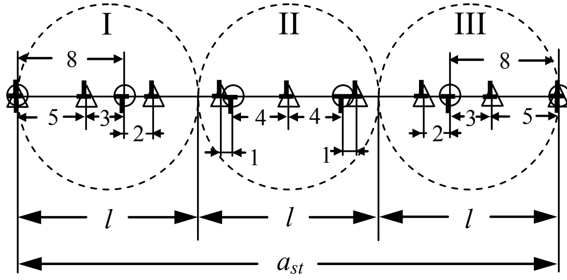

Fig. 3. Schematic depiction of the defect "elementary cell" structure in *n*-InSe/*p*-CdTe heterojunction plane (interactions between dislocations are neglected): triangles – position of the InSe structure elements; empty circles – CdTe elements; ⊥ – misfit dislocations. The numbers denote the distances in 0.81 Å units.

According to [23, 27], the defect of such a complicated structure will create a set of closely-situated acceptor level in the band gap of the base semiconductor, re-distributing the energy in a certain way. To simplify the further analysis, we will assume that this band could be described using an averaged dislocation level with a mean position ΔE_{dis}. Let us also suppose that the electron distribution function at this level f_0^d is governed by the expression [23, 27]

$$f_0^d = \left[1 + g\exp\left(\frac{\Delta E_{\text{dis}} - E_{\text{F}p}}{k_0 T}\right)\right]^{-1}, \qquad (4)$$

with the level degeneration factor equal to

$$g = \frac{m_p k_0 T f}{4\pi^2 \hbar^2 a_n n_0}. \qquad (5)$$

The theoretical parameter f is related to the population of the dislocation level and may vary in the ranges $0.1 \le f \le 0.5$ [23]; all the remaining designations are common. The value of ΔE_{dis} could be found by solving the electro-neutrality equation [23]:

$$\pi \cdot \left(\frac{a_{\text{st}}}{2}\right)^2 \cdot (N_d - N_a) = \frac{f_0^d}{a_{\text{st}}}, \qquad (6)$$

where N_d and N_a are the concentrations of ionized donors and acceptors in the corresponding parts of the space charge region (SCR). It is also assumed that the distance between non-saturated bonds coincides with the translation symmetry period a_{st}, and the radius of dislocation cylinder is equal to $a_{\text{st}}/2$. Substituting (4) in (6), one will obtain:

$$\Delta E_{\text{dis}} = E_{\text{F}p} + k_0 T \cdot \ln\left[\frac{1}{g} \cdot \left(\frac{4}{\pi a_{\text{st}}^3 (N_d - N_a)} - 1\right)\right]. \qquad (7)$$

Using the material and dislocation level parameters mentioned above, and assuming that all the impurity centers are ionized at $T = 300$ K (so that $(N_d - N_a) \approx n_0$ and $f = 0.1$), it is easy to show using formulas (5) and (7) that $g = 28.73$ and $\Delta E_{\text{dis}} = \Delta E_a = 0.39$ eV. The large value of degeneration factor g for energy states confirms their complex structure.

The impurity complex creating the acceptor level is also responsible for formation of a potential barrier $e\varphi_d$, complicating carrier transport via heterojunction. On the other hand, at a certain energy conditions this level may act as recombination or trapping center, in the latter case increasing the effective lifetime τ for the non-equilibrium characters. However, the complex defect structure precludes the first principles calculation of both $e\varphi_d$ and τ. One should also be aware that detected CVC peculiarities for *n*-InSe/*p*-CdTe heterojunction will influence current transport through the junction.

3.2 Mechanisms of current transport in n-InSe/p-CdTe heterojunction

The detailed analysis of the CVC obtained in the framework of abrupt junction model (see, e.g., [28, 29]) revealed that forward-biased ($U < 1$ V) *n*-InSe/*p*-CdTe structure will have both generation-recombination (I_{gr}) and tunneling (I_t) currents. However, we determined voltage ranges when only one of the mechanisms is dominating.

For $0 < U < 0.5$ V, the main current transport mechanism (CTM) is generation-recombination, for which CVC obeys the formula [28]:

$$U = n\frac{k_0 T}{e}\ln\left(\frac{I}{I_{gr}^0} + 1\right), \qquad (8)$$

with the non-ideality coefficient n and cut-off current I_{gr}^0 determined at $U \to 0$ [29]:

$$I_{gr}^0 = S\frac{ed}{\tau}\sqrt{N_C(T) N_V(T)} \exp\left(-\frac{E_g(0)}{nk_0 T}\right). \qquad (9)$$

In the formula (9), the variable d stands for the width of SCR; τ is the effective lifetime of non-equilibrium carriers; N_C and N_V are the density of states in the conduction and valence bands, respectively; S is the effective contact area, and $E_g(0)$ is a band gap value for one of the base semiconductors at $T \to 0$ K.

The CVC for the samples are presented in the half-logarithmic scale in Fig. 4, together with the data calculated for the different temperatures using the formula (8). The resulting figure was used for determination of $n = 3.80 \pm 0.10$; linear fitting of $I_{gr}^0(T)$ (inset to Fig. 4) yielded the activation energy $E_g(0) = 1.36 \pm 0.02$ eV, which correlates well with the data presented in literature $E_g(\text{InSe, 0 K}) = 1.3525$ eV [30].

© 2008, V. Lashkaryov Institute of Semiconductor Physics, National Academy of Sciences of Ukraine

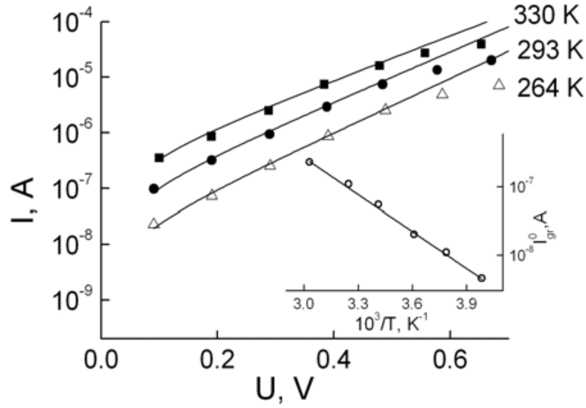

Fig. 4. CVC of *n*-InSe/*p*-CdTe junction under the dominating generation-recombination current transport. The inset shows cut-off current I^0_{gr} versus temperature.

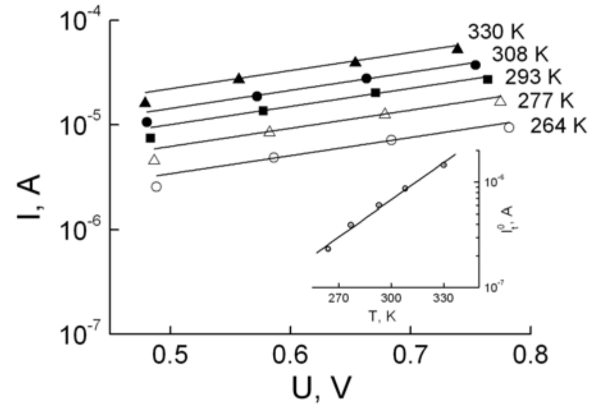

Fig. 5. CVC of *n*-InSe/*p*-CdTe heterojunction under dominating tunneling CTM. The inset presents cut-off current I_{t0} as a function of the temperature.

This result confirms that the most plausible model for generation-recombination processes in the heterojunction studied will include slow recombination centers located at semiconductor junction. Using the formulas (9) with the numerical values (at T = 300 K) $S \approx 0.16$ cm^2, $d \approx 3\cdot10^{-4}$ cm, $E_g(0)/300\, n\, k_0 \approx 14.40$ and the experimentally-determined $I^0_{gr}(300\,\text{K}) \cong 8\cdot10^{-8}\,\text{A}$, the lifetime of non-equilibrium carriers can be calculated as $\tau \approx (5.0\text{-}10)\cdot10^{-5}$ s, which significantly overcomes the relevant value for non-equilibrium electrons in *p*-CdTe ($\tau_n \approx 1.0\cdot10^{-6}$ s [31]), supplying indirect confirmation for the presence of trapping centers at *n*-InSe/*p*-CdTe contact.

For the bias $0.55 < U < 0.80$ V, the set of CVCs for *n*-InSe/*p*-CdTe heterojunction measured at various temperatures and plotted in the semi-logarithmical scale will correspond to parallel lines (Fig. 5), which suggests prevalence of carrier tunneling through the contact [28].

In this case, the experimental CVC can be described by the Neumann empirical formula [28, 29]:

$$I_t = I_{t0}\cdot\exp(\alpha U + \beta T)\,, \tag{10}$$

with the cut-off current $I_{t0} = B\cdot\exp(-\alpha U_d)$ and diffusion potential U_d. The coefficient B = const depends on the characteristics of heterojunction; parameters α and β are independent on voltage and temperature, respectively. For the tunneling CTM, using CVC slopes from semi-logarithmic plots for all temperatures studied, we found that $\alpha = 6.0$ V^{-1}. In this case, the dependence of cut-off current I_{t0} as a function of temperature, plotted in the semi-logarithmic scale (inset to Fig. 5), will be also linear with the slope $\beta = 2.65\cdot10^{-2}$ K^{-1}.

For the bias $U > 0.81$ V, the experimental CVC can be successfully described (Fig. 6) by the expression accounting for the trapping centers (1), characteristic for the prevailing over-barrier current transport [28, 29]:

$$\ln I - \frac{U}{k_0 T} = \ln I_{b0} - \frac{(I/C)^{2/3}}{k_0 T}\,, \tag{11}$$

where I_{b0} is the cut-off current at $U = 0$ with the temperature dependence approximated as [28]:

$$I_{b0} = A\cdot T^2\cdot\exp\left(-\frac{e\varphi_b}{k_0 T}\right). \tag{12}$$

In (12), the value $e\varphi_b$ denotes the height of the potential barrier, and the constant A could be influenced by the type of heterojunction, effective mass of carriers, area of the contact, etc. The slope of $\ln I_{b0} = f(10^3/T)$ (inset to Fig. 6) yields $e\varphi_b = 0.71 \pm 0.03$ eV.

The results presented above and the published electron affinity data for the semiconductors forming the junction allowed construction of the band diagram for *n*-InSe/*p*-CdTe structure for the ideal junction model [16, 28, 29].

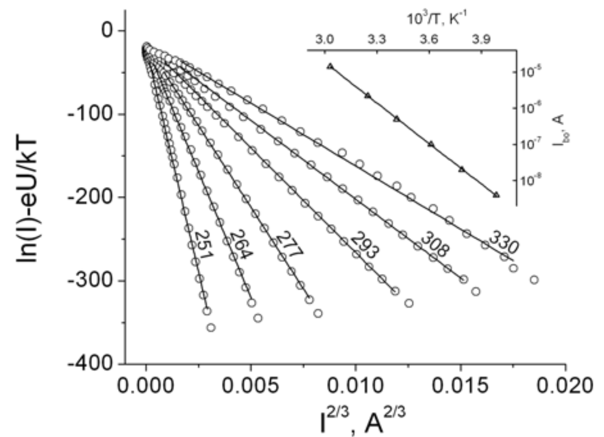

Fig. 6. CVC of *n*-InSe/*p*-CdTe heterojunction under dominating over-barrier current for various temperatures. The inset shows the dependence of cut-off current I_{b0} on the temperature.

© 2008, V. Lashkaryov Institute of Semiconductor Physics, National Academy of Sciences of Ukraine

3.3 Band diagram of n-InSe/p-CdTe heterojunction

According to the Anderson model [28, 29], the potential difference $e\varphi_c$ at the contact is determined by the expression

$$e\varphi_c = (\chi_p + E_{gp} - E_{Fp}) - (\chi_n + E_{Fn}), \quad (13)$$

where χ_p and χ_n are electron affinities of *p*- and *n*-type semiconductors, respectively, E_{gp} is the band gap of *p*-type semiconductor, E_{Fp} is the distance from the valence band top to the Fermi level E_F in *p*-type semiconductor, and E_{Fn} is the distance between the Fermi level and the bottom of conduction band in *n*-type semiconductor. The energy jumps for conduction and valence bands ΔE_C, ΔE_V, width of the space charge region d_n, d_p, and band bending $e\varphi_n$, $e\varphi_p$ in the *n*- and *p*-type semiconductors are given by the formulas:

$$\Delta E_C = \chi_n - \chi_p, \; \Delta E_V = E_{gn} - E_{gp} + \Delta E_C,$$

$$d_n = \sqrt{\frac{2\varepsilon_n \varepsilon_p \varepsilon_0 N_a \varphi_c}{e N_d (\varepsilon_p N_a + \varepsilon_n N_d)}}, \; d_p = \frac{N_d}{N_a} d_n,$$

$$e\varphi_n = \frac{e N_d d_n^2}{2\varepsilon_n \varepsilon_0}, \; e\varphi_p = \frac{e N_a d_p^2}{2\varepsilon_p \varepsilon_0}. \quad (14)$$

Here E_{gn} is the band gap of *n*-type semiconductor; N_d and N_a are the concentration of ionized donors and acceptors in the corresponding areas of SCR; ε_n and ε_p are dielectric constants of the semiconductors forming the junction (ε_0 is a dielectric constant $8.85\cdot10^{-14}$ F/cm), and *e* is the elementary charge. Upon neglecting the barrier $e\varphi_d$ created by misfit dislocations at the junction, one can write down the expressions for $e\varphi_{bn}$ barrier (for the electrons traveling from the conduction band of InSe into that of CdTe) and $e\varphi_{bp}$ barrier (for holes traveling from valence bands of CdTe into that of InSe):

$$e\varphi_{bn} = e\varphi_c + \Delta E_C, \; e\varphi_{bp} = e\varphi_c + \Delta E_V. \quad (15)$$

There is some discrepancy in the values of electron affinities χ_p(CdTe) and χ_n(InSe) in literature: e.g. χ_p = 4.28 eV [28] or 4.30 eV [16]; χ_n = 3.60 eV [32] or 4.55 eV [6, 30]. Our analysis have shown that assuming χ_p = 4.28 eV and χ_p = 4.30 eV one will obtain realistic parameters of the band diagram, while using the value χ_n = 3.6 eV leads to incorrect quantities lacking any qualitative relation to the experimental results concerning the current transport mechanisms in *n*-InSe/*p*-CdTe heterojunction. Table presents the main parameters of the junction, calculated according to the formulas (13)-(15) with χ_n = 4.55 eV and χ_p = 4.30 eV. We have considered the band gap values E_{gp}(CdTe) = 1.47 eV and E_{gn}(InSe) = 1.27 eV for (T = 300 K) following the calculation methodology suggested in Refs. [33, 30] with ε_n = 6.5 [3], ε_p = 10.9 [21], $N_d = n_0 \cong 3\cdot10^{15}$ cm^{-3} and $N_a = p_0 \cong 1\cdot10^{14}$ cm^{-3}. For the sake of comparison, the results obtained for *n*-InSe/*p*-GaSe heterojunctions [4] were also included into Table for χ_n = 4.55 eV, χ_p = 3.6 eV, $E_{Fn} \cong$ 0.17 eV, $E_{Fp} \cong$ 0.18 eV, $N_d = n_0 \cong 5\cdot10^{15}$ cm^{-3}, $N_a = p_0 \cong 1\cdot10^{14}$ cm^{-3}, E_{gn} = 1.27 eV, E_{gp} = 2.02 eV and ε_p = 8.45 [3]. The schematic depiction of the resulting band diagram is shown in Fig. 7.

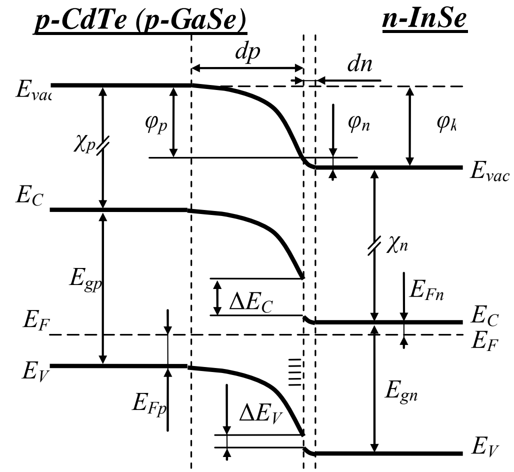

Fig. 7. Schematic band diagram of *n*-InSe/*p*-CdTe and *n*-InSe/*p*-GaSe heterojunctions. The designations are discussed in the text, and the numerical values are presented in Table.

As one can see from the table, for the abrupt junction approximation the parameters of the structure *n*-InSe/*p*-CdTe are determined properly. Under the forward bias for the both heterojunction types, one may get $e\varphi_{bp} < e\varphi_{bn}$, so that over-barrier carrier transport from *p*-type semiconductor to electron material becomes dominating for $U > e\varphi_{bp}$. At the same time, the $e\varphi_c$ values for these junctions are almost equal, while band discontinuities ΔE_C and ΔE_V for *n*-InSe/*p*-CdTe are significantly smaller than those for the *n*-InSe/*p*-GaSe, leading to a significant difference of the barrier heights $e\varphi_{bn}$ and $e\varphi_{bp}$ for the structures studied.

It is important that use of *n*-InSe electron affinity as χ_n =4.55 eV (instead of χ_n = 3.60 eV as it was suggested in the paper [4]) removes a small peak in the band diagram of *n*-InSe/*p*-GaSe heterojunction [4].

If we take into account parameter definition possible errors for the base semiconductor (in particular, concentration and mobility of the majority carriers), than experimentally-derived value for the barrier height $e\varphi_b$ = (0.71 ± 0.03) eV for *n*-InSe/*p*-CdTe could be considered

Table. Parameters of band diagrams for *n*-InSe/*p*-CdTe and *n*-InSe/*p*-GaSe heterojunctions [4].

parameters / results	$e\varphi_c$, eV	ΔE_C, eV	ΔE_V, eV	$e\varphi_n$, eV	$e\varphi_p$, eV	d_n, µm	d_p, µm	$e\varphi_{bn}$, eV	$e\varphi_{bp}$, eV
Our results	0.76	0.25	0.05	0.04	0.72	0.1	2.9	1.01	0.81
Ref. [4]	0.73	0.95	0.20	0.02	0.71	0.08	2.57	1.68	0.93

© 2008, V. Lashkaryov Institute of Semiconductor Physics, National Academy of Sciences of Ukraine

well-correlating with the theoretical predictions $e\varphi_{bp}$ = 0.81 eV, confirming the acceptable accuracy of the suggested band diagram for the heterojunction studied. It is worth mentioning that for *n*-InSe/*p*-CdTe heterojunction for the case of the Anderson model, the distance between the valence band top in the base semiconductors is quite small in comparison with the other heterostructures (see. e.g., [34]), which, in turn, will cause a small difference between $e\varphi_c$ and $e\varphi_{bp}$ (Table). Thus, according to [23] (and also references therein), taking into account for the potential barrier $e\varphi_d$ formed by misfit dislocations will not change the value of $e\varphi_{bp}$, but may increase $e\varphi_{bn}$, introducing significant complication for the carriers tunneling through the contact.

It should be especially emphasized that the obtained parameters of *n*-InSe/*p*-CdTe heterojunction (Table) makes it a perspective competitor of *n*-InSe/*p*-GaSe structure, opening a promising application prospects for the devices operating under high temperatures and radiation.

4. Conclusions

It was successfully proved that the method of deposition over optical contact developed for *n*-InSe/*p*-CdTe heterojunction can form devices similar to *n*-InSe/*p*-GaSe structure. The misfit dislocations at semiconductor junction create a stable translation-symmetry structure, leading to formation of acceptor level located at ΔE_d = 0.39 eV, acting as recombination level or trapping center for non-equilibrium carriers with the lifetimes $\tau \approx (5.0\text{-}10)\cdot 10^{-5}$ s. On the base of temperature analysis of current-voltage curves for the device studied, it was found that the forward-biased (U < 1.5 V) structure *n*-InSe/*p*-CdTe features generation-recombination, tunneling and over-barrier currents. The parameters of aforementioned mechanisms were determined. Using the obtained experimental results in the framework of an ideal heterojunction model, the band diagram for *n*-InSe/*p*-CdTe structure was constructed, predicting promising application perspectives for the junction concerning its stable operation under elevated temperatures and high radiation fluxes.

References

1. V.L. Bakumenko, Z.D. Kovaliuk, L.N. Kurbatov, V.G. Tagiev, V.F. Chishko, Properties of heterojunctions based on indium monoselenide InSe // *Fizika Tekhnika Poluprov.* **12**, p. 374-377 (1978) (in Russian).
2. V.N. Katerynchuk, Z.D. Kovaliuk, V.A. Monasson, K.D. Tovstiuk, About current transport mechanism for GaSe-InSe // *Fiz. Tekhn. Poluprov.* **21**, p. 380-381 (1987) (in Russian).
3. S. Shigetomi, T. Ikari, Electrical and photovoltaic properties of Cu-doped p-GaSe/n-InSe heterojunction // *J. Appl. Phys.* **88**, p. 1520-1524 (2000).
4. S.I. Drapak, V.B. Orletskiy, Z.D. Kovaliuk, Changes of contact potential difference for a heterojunction n-InSe/p-GaSe during the aging process // *Fizika Tekhnika Poluprov.* **38**, p. 566-569 (2004) (in Russian).
5. Z.D. Kovalyuk, V.P. Makhniy, O.I. Yanchuk, Mechanisms of forward current transport in p-GaSe/n-InSe heterojunctions // *Semiconductor Physics, Quantum Electronics & Optoelectronics* **6**, p. 458-460 (2003).
6. O. Lang, A. Klein, C. Pettenkofer, W. Jaegermann, and A. Chevy, Band lineup of lattice mismatched InSe/GaSe quantum well structures prepared by van der Waals epitaxy: Absence of interfacial dipoles // *J. Appl. Phys.* **80**, p. 3817-3821 (1996).
7. W.H. Schlesinger, Semiconductors for room temperature nuclear detector applications // *Semiconductors and semimetals* **43**, Lavoisier (1995).
8. *Wide-band Layered Crystals and Their Physical Properties*, A.B. Liskovich (Ed.). Lviv University, Lviv, 1982 (in Russian).
9. N.N. Berchenko, V.E. Krevs, V.G. Sredin, *Semiconductor Solid Solutions and Their Applications.* Voenizdat, Moscow, 1982 (in Russian).
10. M. Persin, B. Pivac, N. Urli, S. Popovich, F. Cavdarbasa, Some electrical properties of an n-InSe/p-CdTe heterojunction // *Fizika (SFRJ)* **16**, p. 279-284 (1984).
11. Z.D. Kovalyuk, O.A. Politans'ka, Creation and investigation of p-n-junctions p-InSe⟨Cd⟩ using pulsed laser radiation // *Fizika i Khimiya Tverdogo Tela* **6**, p. 146-148 (2005) (in Russian).
12. G.L. Belen'kij, Ye.Yu. Salaev, R.A. Sulejmanov, Deformation phenomena in the layered crystals // *Uspekhi Fizicheskikh Nauk* **155**, p. 89-127 (1988) (in Russian).
13. K.Z. Rushchanskiy, Influence of the hydrostatic pressure on static and dynamic properties of InSe crystals: first-principle studies // *Fizika Tverdogo Tela* **46**, p. 177-184 (2004) (in Russian).
14. Zh. Pankov, *Optical Processes in Semiconductors*, Zh.I. Alferov and V.S. Vavilov (Eds.). Mir, Moscow, 1973 (in Russian).
15. H.J. Moller, *Semiconductors for Solar Cells*. Boston-London, Atrech House, 1993.
16. S.J. Fonash, *Solar Cell Devices Physics*. New York, Academic Press, 1981.
17. Ya.S. Mazurkevych, A.G. Voloshchuk, S.B. Kosenkov, G.G. Grushka, Method of chemical surface treatment of the tellurium-containing semiconductor materials, *Patent № 1080680* (1983).
18. P.P. Horley, O.A. Chervinskiy, Software for investigations of current transport in semiconductor structures // *Sensor Electronics and Microsystem Technologies* **23** (4), p. 16-20 (2007).
19. E.I. Adirovich, P.M. Karageorgiy-Alkalaev, A.Yu. Leiderman, *Double Injection Current in Semiconductors*. Sovetskoe Radio, Moscow, 1978 (in Russian).

© 2008, V. Lashkaryov Institute of Semiconductor Physics, National Academy of Sciences of Ukraine

20. P.M. Karageorgiy-Alkalaev, A.Yu. Leiderman, *Deep Impurity Levels in Wide-band Semiconductors.* F.A.N., Tashkent, 1971 (in Russian).
21. A.V. Savitskiy, *Manufacturing and Physical Properties of Cadmium Telluride.* U.M.K. V.O., Kiev, 1990 (in Russian).
22. J.L. Pautrat, J.M. Francou, N. Magnea, E. Molva, K. Saminadayar, Donors and acceptors in tellurium compounds; the problem of doping and self-compensation // *J. Cryst. Growth* **72**, p. 194-204 (1985).
23. G. Matare, *Electronics of Defects in Semiconductors*. Mir, Moscow, 1974 (in Russian).
24. A. Kelli, G. Grows, *Crystallography and Defects in the Crystals*. Mir, Moscow, 1974 (in Russian).
25. J. Hirt, I. Lote, *Dislocation Theory*. Atomizdat, Moscow, 1972 (in Russian).
26. V.T. Rid, *Dislocations in the crystals*. Metallurgizdat, Moscow, 1957(in Russian).
27. V.I. Fistul', *Introduction to Semiconductor Physics*. Vysshaya Shkola, Moscow, 1975 (in Russian).
28. B.L. Sharma, P.K. Purokhit, *Semiconductor Heterojunctions*. Mir, Moscow, 1979 (in Russian).
29. S.M. Sze. *Physics of Semiconductor Devices*. Energiya, Moscow, 1973 (in Russian).
30. J. Camassel, P. Merle, H. Mathieu, A. Chevy, Excitonic absorption edge of indium selenide // *Phys. Rev. B.* **17**, p. 4718-4725 (1978).
31. E.S. Ortobolevskaya, E.A. Afanas'eva, L.K. Vodop'yanov, V.P. Sushkov, *Cadmium Telluride*, V.M. Wool (Ed.). Nauka, Moscow, 1968, p. 97-102 (in Russian).
32. J. Martinez-Pastor, A. Segura, J.L. Valdes, and A. Chevy, Electrical and photovoltaic properties of indium-tin-oxide/p-InSe/Au solar cells // *J. Appl. Phys.* **62**, p. 1477-1483 (1987).
33. S. Yamanaka, S. Tsushima, H. Shimizu and Y. Tokumary, Temperature dependence of photocurrent and band gap of Cl-doped semi-insulating CdTe with evaporated Au electrodes // *Jpn J. Appl. Phys.* **41**, p. 5538-5541 (2002).
34. A. Waag, Y.S. Wu, R. Bicknell-Tassius, C. Gonser-Buntrock, and G. Landwehr, Investigation of molecular-beam epitaxially grown CdTe on GaAs by x-ray photoelectron spectroscopy // *J. Appl. Phys.* **68**, p. 212-217 (1990).

© 2008, V. Lashkaryov Institute of Semiconductor Physics, National Academy of Sciences of Ukraine